Automated Extraction of Paper Watermarks

Paul F Whelan[1] and Pierre Soille[2]

[1] Vision Systems Laboratory
School of Electronic Engineering
Dublin City University
Dublin 9, Ireland
whelanp@eeng.dcu.ie
[2] LGI2P, Ecole des Mines d'Alès
Parc scientifique Georges Besse
F-30000 Nîmes, France
Pierre.Soille@eerie.fr

Abstract. The aim of this paper is to outline the issues involved in the application of machine vision to the automatic extraction of watermarks from paper samples. The correct identification and localisation of watermarks is a key issue in paper manufacturing. As well as requiring the position of the watermark for defect detection and classification, it is necessary to insure its position on the paper prior to the cutting process. Two paper types are discussed, with and without laid and chain lines (these lines appear as a complex periodic background to the watermark and further complicate the segmentation process). We will examine both morphological and Fourier approaches to the watermark segmentation process, concentrating specifically on those images with complex backgrounds. Finally we will compare and contrast these approaches.

Keywords: Watermark, Paper, Machine Vision, Morphology, Fourier.

1 Introduction

Watermarks are generally used for security and quality purposes. They take the form of brand names, brook bonds or logos (Figure 1). They are typically formed by a pressing process using a metal stamp containing an impression of the desired pattern. This pattern induces a variation in the paper thickness and is implemented at the end of the wet stage of the paper production process. Currently, the watermark is captured on-line and displayed on a CRT beside an image of a good sample, where operators examine it occasionally. This enables the identification of gross errors, whereas the operators classify other defects on a subjective basis. Our aim is to automate the watermark registration as the first phase in the defect detection and classification process. Key to the success of this operation is the reliable segmentation of the watermark for plain and non-plain paper types. Non-plain paper samples contain laid and chain lines (Figure 1b). The horizontal *laid lines* are due to the wire mesh that was used to hold the paper during fabrication [1]. The vertical *chain lines* are due to the thicker wire that was used to support the laid lines. The localisation of the watermark is also critical to the paper cutting operation, since some manufacturers require the watermark to appear in the same location on each cut sheet.

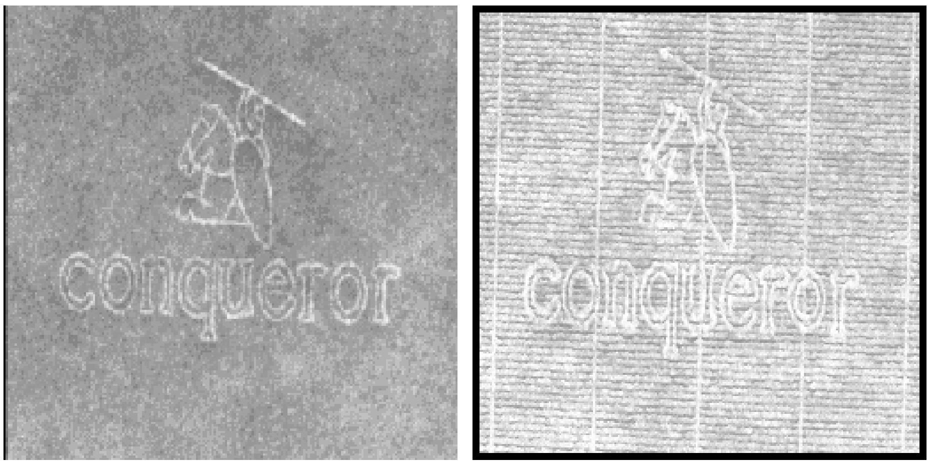

(a) Plain paper, i. e. without chain and laid lines.

(b) Non-plain paper, i. e. with chain (vertical) and laid (horizontal) lines.

Fig. 1. A typical watermark on (a) plain paper and (b) paper with chain and laid lines. Note the uneven illumination on both images.

This paper is organised as follows. Section 2 details the image acquisition and the resulting image characteristics. It also refers to previous works reporting techniques for extracting watermarks. Our approach for processing watermarks on plain paper is presented in Sec. 3. More sophisticated techniques allowing the extraction of watermarks on non-plain paper are proposed in Sec. 4. Before concluding, we give in Sec. 5 some guidelines about a possible real-time implementation of the proposed methodology.

2 Background

2.1 Development Environment

The laboratory development system used for the initial phase of this project consisted of the following elements:

- Sony XC 77CE monochrome CCD array camera with a 25 mm Cosmicar lens.
- A Lightbox to provide the diffuse backlighting necessary to illuminate the watermark.
- A PC resident ITI frame grabber. All images were stored as grey level TIFF images.
- MvT16 - A windows based Machine Vision software development environment resident on a PC [2].
- Xliiar, a Library of Independent Image Analysis Routines [3] linked to Xlisp [4], an experimental lisp interpreter.

A key problem with the development system has been producing a even light profile across the image. While the morphological top-hat discussed in Sec. 3.1 can be used to reduce or eliminate a lighting gradient, we would prefer to reduce, or if possible prevent, this problem from occurring. It is envisaged that the production system will use a backlighting strip in conjunction with a high resolution linescan CCD camera (see Sec. 5). The design of the lighting system would be such as to reduce the uneven illumination that can occur across the width of the image.

2.2 Previous works

Techniques for capturing digital images of historical watermarks are developed in [5]. The authors propose to capture the images in both transmitted and reflected light so as to discriminate watermark from ink information. The extraction of watermarks on old *hand-written* documents is detailed in [6]. The management of a multimedia database of historical papers representing ancient watermarks is detailed in [1]. We found no published report dealing with the on-line detection and registration of watermarks in paper manufacturing.

3 Plain Paper

Global thresholding cannot be reliably used for extracting watermarks on plain paper. This is due to both the uneven illumination function and the very low contrast of the watermark itself. For example, the direct thresholding of the watermark on plain paper shown in Fig. 1a is shown in Fig. 2.

Since the watermarks appear as a network of thin crest lines, techniques designed for extracting thin nets such as those based on the maximal curvature [7] have proven their effectiveness. However, this approach is hampered by a very high computation load which makes it unsuitable for a machine vision application (the paper web speed is 300 meters per minute). Keeping in mind the speed constraints, we found that a morphological white top-hat transform followed by a double threshold and some additional cleaning filters is the best solution.

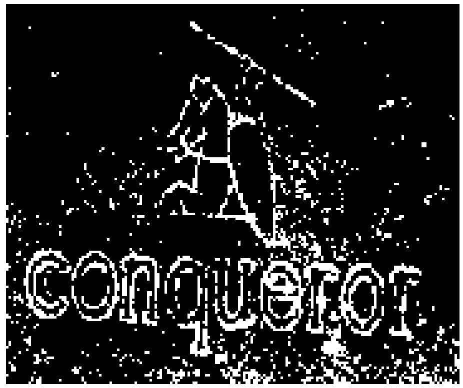

Fig. 2. Direct thresholding of the watermark image shown in Fig. 1a.

3.1 White Top Hat Transformation

The choice of a given morphological filter is usually driven by the available knowledge about the shape, size, and orientation of the structures one would like to filter out or extract [8]. For example, we may choose an opening by a 2×2 square structuring element (SE) to remove positive impulse noise or a union of openings with line segments to extract elongated bright image structures. Morphological top-hats proceed *a contrario*. Indeed, the approach undertaken with top-hats consists in using knowledge about the shape characteristics that are *not* shared by the relevant image structures. An opening with a SE that does not fit the relevant image structures is then used to *remove* them from the image. These structures are recovered through the arithmetic difference between the image and its opening. This operation is called white top-hat or top-hat by opening [9].

Since the watermark consists of a network of thin lines, we have to consider an opening with a square slightly larger than the width of these lines. The opened image provides us with the illumination function which is then subtracted from the original image to enhance the watermark. This procedure is illustrated in Fig. 3.

3.2 Double threshold

The *double threshold operator* $DBLT$ thresholds the input image for two ranges of grey scale values, one being included in the other. The threshold T for the narrow range is then used as a seed for the reconstruction of the threshold for the wide range:

$$DBLT_{[t_1 \leq t_2 \leq t_3 \leq t_4]}(f) = R_{T_{[t_1,t_4]}}[T_{[t_2,t_3]}(f)],$$

where R denotes the morphological reconstruction by dilation [10, 11]. The resulting binary image is much cleaner than that obtained with a unique threshold.

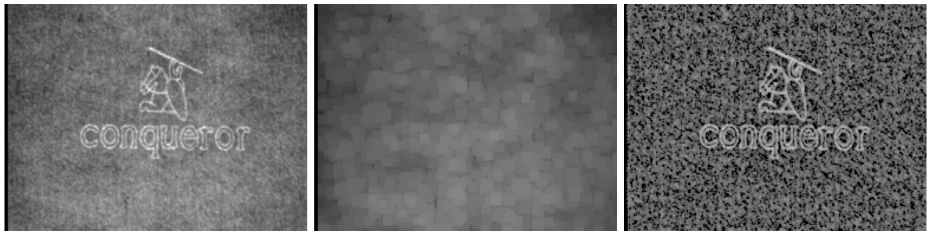

(a) Input image (b) Opening with a 7 × 7 square (c) White top-hat: arithmetic difference between (a) and (b)

Fig. 3. From uneven to even background using the white top-hat transform.

Moreover, the result is more stable to slight modifications of threshold values. The double threshold technique is very similar to the *hysteresis threshold* proposed in [12].

The final filtering stage is based on a surface area criterion applied to the closing of the double threshold image: all connected components having a number of pixels smaller than a given threshold are removed. The filtered closed image is then intersected with the double threshold image. The whole procedure is illustrated in Fig. 4, starting from the top-hat image shown in Fig. 3c.

4 Paper with Laid and Chain Lines

If we perform a white top-hat and a threshold on non-plain papers, we extract the watermark and the laid/chain lines. (This is due to the fact that the both the lines and the watermark are of similar intensity). The problem is to remove these lines so as to output a clean mask of the watermark. We have explored two different approaches: the first is based on the Fourier transform and the second uses morphological operators.

4.1 Fourier based Segmentation

The Two-dimensional Discrete Fourier Transform (DFT) is a powerful tool in the extraction of periodic information in digital image processing applications. The DFT is the sampled Fourier Transform and therefore does not contain all frequencies forming an image, but only a set of samples which is large enough to fully describe the real domain image. This operation allows spatial periodicities in the intensity within an image to be investigated, in order to find, amongst other features, the dominant frequencies. The number of frequencies corresponds to the number of pixels in the real domain image, i.e. the image in the real and Fourier space are of the same size.

Several algorithms have been developed to calculate the two-dimensional DFT. The simplest makes use of the observation that this is a separable transform which can be computed as a sequence of two one-dimensional transforms. Therefore, we can generate the two-dimensional transform by calculating the

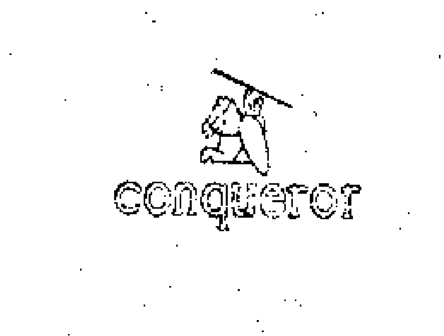

(a) First threshold of white top-hat: marker image

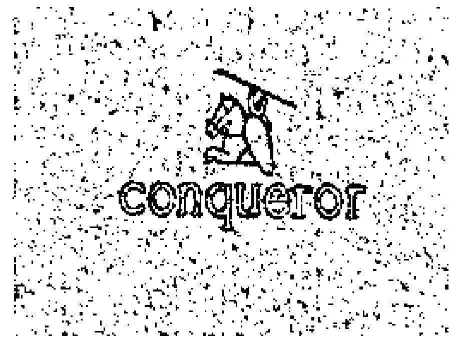

(b) Second threshold of white top-hat: mask image

(c) Reconstruction of (b) from (a)

(d) After filtering based on the surface area of the connected component of the closing of (c) by a 3 × 3 SE

Fig. 4. Extraction of the watermark from the white top-hat image shown in Fig. 3c: double threshold and additional filtering.

one-dimensional DFT along the image rows and then repeating this on the resulting image but, this time, operating on the columns. This reduces the computational overhead when compared to direct two-dimensional implementations.

Although this is still computationally slow compared to other many segmentation techniques, the Fourier transform is quite powerful. It allows the input to be represented in the frequency domain, which can be displayed as a pair of images. (It is not possible to represent both amplitude and phase using a single monochrome image.) Once the processing within the frequency domain is complete, the inverse transform can be used to generate a new image in the original, so-called, spatial domain. The Fourier power, or amplitude, spectrum plays an important role in image processing and analysis. This can be displayed, processed and analysed as an intensity image. Fortunately this is not just an algorithmic transformation but a physical one. The FT can be implemented real time using optical techniques [13, 14].

The periodic nature of the laid and chain lines indicates the possibility of examining and filtering the paper images in the Fourier domain. To remove laid and chain lines, the filter design must contain *a priori* knowledge about the line properties. The images are transformed in to the Fourier domain using the DFT (Fig. 5). Due to their higher frequency, the laid lines appear as distinctive frequency spectrum peaks in this domain, see Fig. 5(b). The lower frequency chain lines are not as obvious, since they are hidden by the significant amount of low frequency information in the image. An adaptive low pass filter (based on applying a filter to the DFT power spectrum (spectral density)) is applied to the resultant image to remove these peaks.

When the inverse FT is applied to this image we are left with a representation of the laid and chain line data. A difference image is formed by subtracting the extracted lines from the original image to produce the segmentation of the watermark. The white top-hat transformation (Sec. 3.1), thresholding and filtering (Sec. 3.2) stages are then applied to the resultant segmented image. Finally we apply a mask to eliminate boundary pixels. This procedure is illustrated in Fig. 5. While the resultant image has been degraded, we are left with sufficient information to allow us to register the watermark on the paper sheet.

Alternatively, a selective low-pass filter can be applied locally to the high frequency peaks, representing the laid lines, in the Fourier spectrum. This procedure is illustrated in Fig. 6. While this process is more efficient at removing the laid lines, the chain lines are clearly visible. But, as we shall discuss in Sec. 5 the chain lines can be detected and masked out from the image.

4.2 Morphology based segmentation

The idea here is to design a morphological filter for extracting the laid and chain lines. We perform a horizontal opening with a long line segment for extracting the laid lines (a morphological opening consists in performing an erosion followed by a dilation with the transposed SE). An opening with a vertical line segment allows us to extract the vertical chain lines. The union of both images is still an

(a) Original Image.

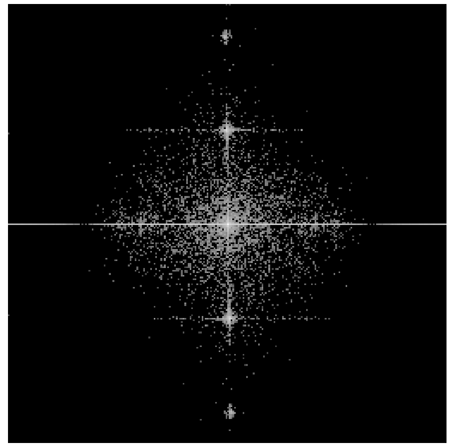

(b) Discrete Fourier Transform frequency spectrum as an intensity function.

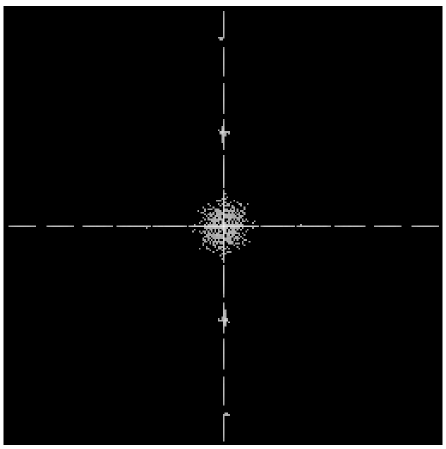

(c) Frequency spectrum of an adaptive low pass filter applied to (b).

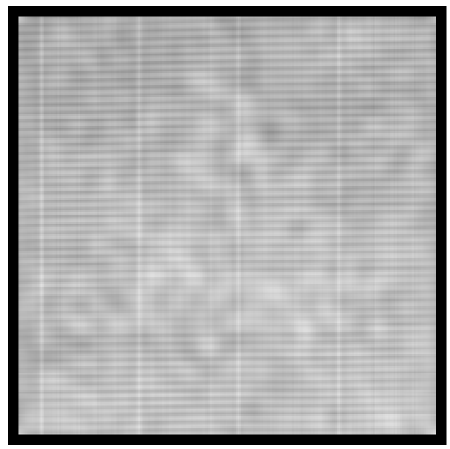

(d) Inverse Fourier Transform of (c).

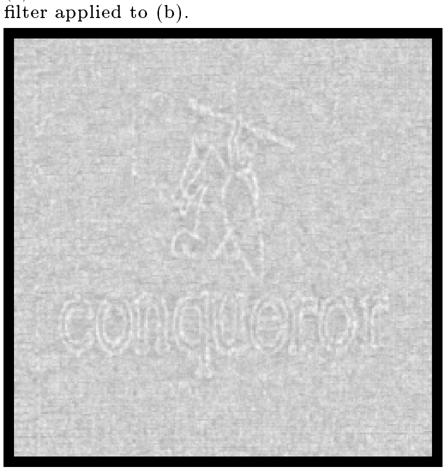

(e) Difference image when (d) is subtracted from the original image (a).

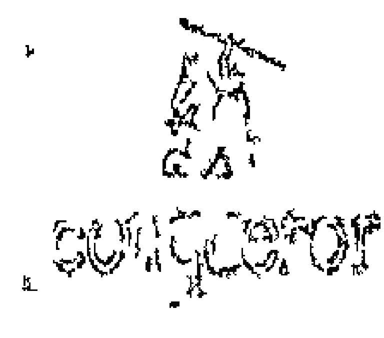

(f) Filtered double threshold of (e).

Fig. 5. The application of the DFT to non-plain paper samples.

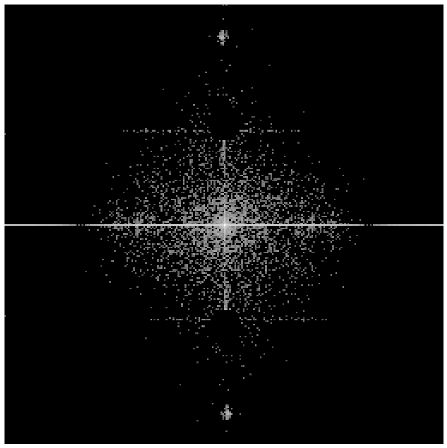

(a) Selective low-pass filtering of Fig. 5 (a).

(b) Inverse Fourier Transform of (a).

(c) White top-hat of (b).

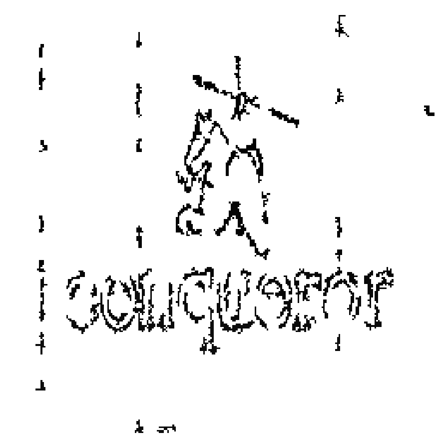

(d) Filtered double threshold of (c).

Fig. 6. Selective low-pass filtering of the Fourier Transform.

opening. This is a well known theorem in morphology: any point-wise maximum of a series of openings is itself an opening [15].

In our application, a morphological opening with long line segments is too sensitive to small gaps along the lines we would like to extract. An efficient solution to this problem is to consider a parametric opening which is not as 'strong' as the corresponding morphological opening. Rather than using a line structuring element of n pixels, we consider all subsets of this structuring element which contains only k pixels ($k < n$). The parametric opening is then defined as the union (or point-wise maximum $\vee$ for grey scale images) of the morphological openings with these SEs:

$$\gamma_{L_{n,k}}(f) = \bigvee_i \{\gamma_{B_i} \mid B_i \cup \{p_1, \ldots, p_{n-k}\} = L_n\}.$$

Fortunately, we do not need to compute all morphological openings in parallel[1] since it can be shown that the union of all these openings equals the point-wise minimum operator $\wedge$ between (i) the original image f and (ii) the dilation δ with the full line segment L_n of the rank filter of the original image using the full line segment as mask and selecting the rank k:

$$\gamma_{L_{n,k}}(f) = f \wedge \delta_{L_n}[\mathrm{Rank}^k_{L_n}(f)].$$

Once the parametric opening has been computed, we subtract it from the original image so as to enhance the watermark (it is therefore another white top-hat transform). We then threshold the white top-hat and perform additional cleaning filters (i.e. using the filtering process discussed in Sec. 3.2). The proposed steps for the morphological processing of non-plain paper are illustrated in Fig. 7.

The computation load of the opening step is reduced when using the fast recursive algorithm detailed in [16] for the morphological dilation and the moving histogram technique [17] for computing the rank filter.

5 Proposed Real-time Implementation

We can assume that the orientation of the watermark is always the same compared to the vertical chain lines. Also, we know that the direction of movement of the paper is the same as the chain lines. This leads us to propose a real-time implementation based on the preceding discussion. (It should be emphasised that this approach has not yet been implemented, and as such results cannot be presented).

1. While the line scan camera acquires the image, we compute the running sum of the grey level along the image columns so as to detect the chain lines (of course the vertical lines may deviate from an ideal vertical direction but

[1] There are $\frac{n!}{k!(n-k)!}$ such openings.

(a) Input image.

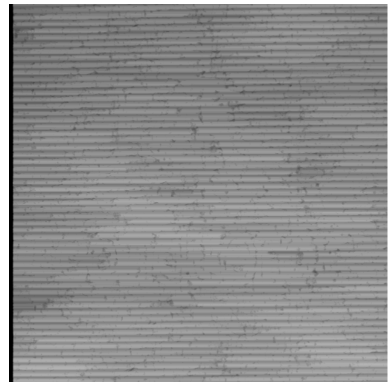

(b) Horizontal parametric opening.

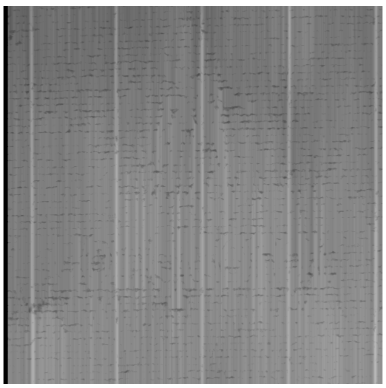

(c) Vertical parametric opening.

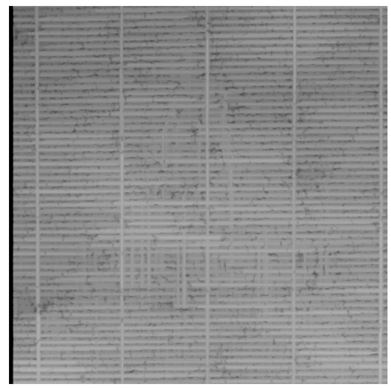

(d) Union of the two openings.

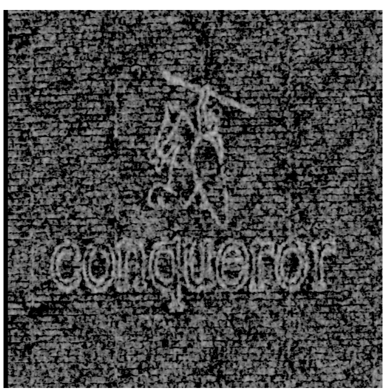

(e) Subtraction of the opening (d) from the original image (a).

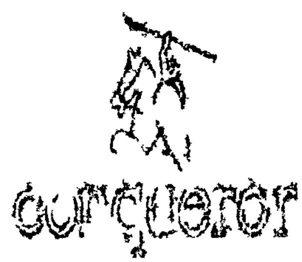

(f) Filtered double threshold of (e).

Fig. 7. Morphology based processing of watermarks on non-plain paper containing laid and chain lines.

we can get around this problem by determining their actual direction and computing the sum along the corresponding discrete line, readjusting the direction after each line acquisition).
2. Now we assume that the horizontal laid lines are horizontal enough so as to allow for a parametric opening along the lines acquired by the camera. If the horizontal lines are always perfectly perpendicular to the vertical lines, we could use openings along the direction perpendicular to that computed in step 1.
3. We subtract the opening from the input image (top-hat like transform). The resulting image contains high grey scale values for the watermark and the vertical lines.
4. By computing the sum of the grey scale levels along the lines and the columns of the image derived from step 3, we can determine the orientation, position, and magnification factor of the watermark. It can be then extracted by comparing the actual image with the corresponding ideal watermark image.

6 Conclusions

Fourier and morphology based segmentation of non-plain papers have been proposed. While both approaches performed well under our limited testing, the morphological based segmentation produces slightly better results and is better suited to a real-time implementation. The work described in this paper is part of an ongoing project. Further testing needs to be carried out on a larger database of sample images to obtain the optimum set of parameters that will ensure the maximum performance of the segmentation process.

7 Acknowledgements

We would like to express our gratitude to Rafael Carmona for his initial work on this project. We would also like to thank *Technology Systems International Ltd. (Dublin)* for their support.

References

1. C. Rauber, P. Tschudin, S. Startchik, and T. Pun, "Archival and retrieval of historical watermark images," in *International Conference on Image Processing (ICIP)*, Lausanne, 1996, pp. 773–776, IEEE Press.
2. B. Batchelor and P. Whelan, *Intelligent vision systems for industry*, Springer-Verlag, London, 1997.
3. E. Breen, P. Soille, C. Skelsey, L. Bischof, and H. Talbot, "The LIAR project," URL: **http://www.dms.csiro.au/~edb/liarProject/liar.html**, 1996.
4. D. Betz, "An XLISP tutorial," *Byte*, 1895.
5. D. Stewart, R. Scharf, and J. Arney, "Techniques for digital image capture of watermarks," *Journal of Imaging Science and Technology*, vol. 39, no. 3, pp. 261–267, June 1994.

6. P. Zamperoni, "Wasserzeichenextraktion aus digitalisierten Bildern mit Methoden der digitalen Bildsignalverarbeitung," *Das Papier*, vol. 43, no. 4, pp. 133–143, 1989.
7. O. Monga, N. Armande, and Ph. Montesinos, "Thin nets and crest lines: Application to satellite data and medical images," *Computer Vision and Image Understanding*, vol. 67, no. 3, pp. 285–295, September 1997.
8. P. Soille, *Morphologische Bildverarbeitung*, Springer-Verlag, Berlin Heidelberg, 1998.
9. F. Meyer, "Automatic screening of cytological specimens," *Computer Vision, Graphics, and Image Processing*, vol. 35, pp. 356–369, 1986.
10. C. Lantuéjoul and F. Maisonneuve, "Geodesic methods in image analysis," *Pattern Recognition*, vol. 17, no. 2, pp. 177–187, 1984.
11. P. Soille, "Geodesic transformations and metrics: an overview," in *Brazilian Workshop'97 on Mathematical Morphology, mini-course II*, G. Banon, Ed., CP 515, CEP 12201-970 São José dos Campos, SP, Brazil, February 1997, Instituto Nacional de Pesquisas Espaciais, pp. 1–48.
12. J. Canny, "A computational approach to edge detection," *IEEE Transactions on Pattern Analysis and Machine Intelligence*, vol. 8, no. 6, pp. 679–698, November 1986.
13. H. Stark, *Applications of Optical Fourier Transforms*, Academic Press, 1982.
14. G.A. Betzos P.A. Mitkas and L.J. Irakliotis, "Optical processing paradigms for electronic computers," *IEEE Computer*, vol. 31, no. 2, pp. 45–51, Feb 1998.
15. G. Matheron, *Eléments pour une théorie des milieux poreux*, Masson, Paris, 1967.
16. P. Soille, E. Breen, and R. Jones, "Recursive implementation of erosions and dilations along discrete lines at arbitrary angles," *IEEE Transactions on Pattern Analysis and Machine Intelligence*, vol. 18, no. 5, pp. 562–567, May 1996.
17. T. Huang, G. Yang, and G. Tang, "A fast two-dimensional median filtering algorithm," *IEEE Transactions on Acoustics, Speech and Signal Processing*, vol. 27, no. 1, pp. 13–18, February 1979.